Title

PET Imaging of Neuropathology in Tauopathies: Progressive Supranuclear Palsy



Journal

Journal of Alzheimer's Disease, 36(1)

ISSN

1387-2877

Authors

Kepe, Vladimir

Bordelon, Yvette

Boxer, Adam

et al.

Publication Date

2013

DOI

10.3233/jad-130032

Peer reviewed

Published in final edited form as:
*J Alzheimers Dis*. 2013 January 1; 36(1): 145–153. doi:10.3233/JAD-130032.

# PET Imaging of Neuropathology in Tauopathies: Progressive Supranuclear Palsy

**Vladimir Kepe, PhD**[a], **Yvette Bordelon, MD, PhD**[b], **Adam Boxer, MD, PhD**[e], **Sung-Cheng Huang, DSc**[a], **Jie Liu, PhD**[a], **Frederick C. Thiede, BSc**[b], **John C. Mazziotta, MD, PhD**[b], **Mario F. Mendez, MD, PhD**[b,c,f], **Natacha Donoghue, MA**[c,d], **Gary W. Small, MD**[c], and **Jorge R. Barrio, PhD**[*]

[a]Department of Molecular and Medical Pharmacology, David Geffen School of Medicine, University of California at Los Angeles, Los Angeles, CA 90095

[b]Department of Neurology, David Geffen School of Medicine, University of California at Los Angeles, Los Angeles, CA 90095

[c]Department of Psychiatry and Biobehavioral Sciences, David Geffen School of Medicine, University of California at Los Angeles, Los Angeles, CA 90095

[d]Semel Institute for Neuroscience and Human Behavior, David Geffen School of Medicine, University of California at Los Angeles, Los Angeles, CA 90095

[e]Memory and Aging Center, Department of Neurology, University of California, San Francisco, CA 94143-1207

[f]VA Greater Los Angeles Healthcare Center, Los Angeles, CA

## Abstract

**Objective—**Currently [F-18]FDDNP is the only PET imaging probe with the ability to visualize hyperphosphorylated tau fibrillar aggregates in living subjects. In this work, we evaluate *in vivo* [F-18]FDDNP labeling of brain neuropathology, primarily tau fibrillar aggregates, in patients with progressive supranuclear palsy (PSP), a human tauopathy usually lacking β-amyloid deposits.

**Methods—**Fifteen patients with PSP received [F-18]FDDNP PET scanning. [F-18]FDDNP distribution volume ratios (DVR), in reference to cerebellar gray matter, were determined for cortical and subcortical areas and compared with those of patients with Parkinson's disease (PD) with short disease duration, and age-matched control subjects without neurodegenerative disorders.

**Results—**[F-18]FDDNP binding was present in subcortical areas (e.g., striatum, thalamus, subthalamic region, midbrain and cerebellar white matter) regardless of disease severity, with progressive subcortical and cortical involvement as disease severity increased. Brain patterns of [F-18]FDDNP binding were entirely consistent with the known pathology distribution for PSP.

[*]Address Correspondence to: Jorge R. Barrio, PhD, David Geffen School of Medicine at UCLA, Department of Molecular and Medical Pharmacology, CHS B2-086A, 694817, 10833 Le Conte Avenue, Los Angeles, CA 90095-6948. jbarrio@mednet.ucla.edu, phone: 310-825-4167; fax: 310-825-4517.

**Contributors.** VK, YB, AB, SCH, JCM, MFM, GWS, JRB designed the study. YB, AB, MFM, FT, ND, GWS recruited and evaluated subjects. JL performed radiosynthesis. VK analyzed the imaging data. VK, YB, SCH, MFM, GWS and JRB interpreted the data. VK, YB, JL, MFM, and JRB prepared the initial manuscript. All authors contributed to the final version of the manuscript.

**Conflict of Interest.** The University of California, Los Angeles (UCLA), owns a U.S. patent, "Methods for Labeling β-Amyloid Plaques and Neurofibrillary Tangles" (6,274,119), that uses the approach outlined in this article. Drs. Huang, Small, and Barrio, are listed among the inventors. All other authors report that they have no conflict of interest.

High midbrain and subthalamic region [F-18]FDDNP binding was distinctive for PSP subjects and separated them from controls and patients with PD.

**Conclusions—**These results provide evidence that [F-18]FDDNP is a sensitive *in vivo* PET imaging probe to map and quantify the dynamic regional localization of tau fibrillar aggregates in PSP. Furthermore, [F-18]FDDNP PET may provide a tool to detect changes in tau pathology distribution either associated with disease progression or as a treatment biomarker for future tau-specific therapies. Patterns of [F-18]FDDNP binding may also be useful in diagnosis early in disease presentation when clinical distinction among neurodegenerative disorders is often difficult.

### Keywords

Key-words: positron emission tomography; FDDNP; progressive supranuclear palsy; Parkinson's disease; neuropathology; hyperphosphorylated tau aggregates; tauopathy

## INTRODUCTION

*In vivo* imaging of neuropathological insoluble protein aggregates with positron emission tomography (PET) can aid in early diagnosis of neurodegenerative diseases before extensive neuronal loss and clinical symptoms become evident [1]. It can also serve as an indicator of treatment efficacy for interventions aimed at preventing or slowing protein aggregate deposition if it possesses sufficient sensitivity to detect changes in protein lesion loads resulting from disease progression or from effective targeted therapies.

During the last decade, investigators have introduced numerous imaging probes with purported specificity for β-amyloid plaques, [C-11]PiB, [F-18]3′-fluoro-PiB ([F-18]flutemetamol, [C-11]SB-13, [F-18]BAY94-9172 ([F-18]florbetaben), [F-18]AV45 ([F-18]florbetapir), BF-227, among others [2]; however, only 2-(1-{6-[(2-[F-18]fluoroethyl)(methyl)amino]-2-naphthyl}ethylidene)malononitrile ([F-18]FDDNP) has been shown capable of detecting tau protein deposits in the living human brain. [F-18]FDDNP is specific for the β-pleated sheet conformation present in amyloid fibrils of all types, both *in vitro* [3] and *in vivo* in Alzheimer's disease (AD) and mild cognitive impairment [4,5], in Gerstmann-Sträussler-Scheinker disease and other prion diseases [6,7], as well as tau neuropathology in fronto-temporal lobe dementia (FTLD) [8]. [F-18]FDDNP PET in AD has shown a pattern of cortical binding that includes both β-amyloid senile plaque (SP) and hyperphosphorylated tau neurofibrillary tangle (NFT) rich areas of the AD brain compared with no cortical binding in cognitively normal controls [4,5]. Recently, a number of [F-18]fluorinated molecular imaging probes have shown *in vitro* ability to label tau aggregates and to possess selectivity for tau over β-amyloid aggregates, *i.e.* THK523 [9, 10] and T807 [11], and they are now being evaluated for human use with PET [12, 13].

The ability of [F-18]FDDNP to label fibrillar tau in NFT rich areas in AD points to its potential as an *in vivo* tau marker in neurodegenerative disorders characterized by tau pathology, usually in the absence of β-amyloid aggregates. These disorders include progressive supranuclear palsy (PSP), corticobasal degeneration (CBD), FTLD with tau pathology, and argyrophilic grain disease [14]. Of these, PSP offers an excellent human model of brain tauopathies for evaluation of [F-18]FDDNP PET for *in vivo* detection of fibrillar tau aggregates in subcortical, and in some cases, also cortical areas of the brain. In contrast to AD, where fibrillar tau is found predominately in the form of neuronal NFTs in the cortex, tau fibrillar aggregates in PSP occur in neurons (NFTs), astrocytes (tuft-shaped astrocytes) and oligodendrocytes (coiled bodies) in both cortical and subcortical regions [15, 16].

With this work we tested the hypothesis that 1) [F-18]FDDNP PET is a sensitive *in vivo* imaging method for neurodegenerative tau lesions in PSP patients; and 2) [F-18]FDDNP brain regional deposition in these patients will be increased in subcortical and cortical areas known to have progressive deposition of tau pathology. Comparison was made with another neurodegenerative disorder with similar clinical symptomatology early on in disease course, Parkinson disease (PD). Lewy body pathology characteristic of PD, and also detected *in vitro* by FDDNP based on the fibrillar structure of α-synuclein aggregates, present different brain distribution patterns and lower densities than tau pathology in PSP. This allows separation of these two conditions based on their distinctive *in vivo* [F-18]FDDNP brain binding patterns.

## MATERIALS AND METHODS

Written, informed consent was obtained from subjects in accordance with procedures of the Office of the Human Research Protection Program (OHRPP) of the University of California, Los Angeles, under strict, standard ethics guidelines. Capacity to provide informed consent was determined for each subject in the presence of a spouse or caregiver by questioning the subject's understanding of key elements of the study including risks and benefits. If a subject was deemed not able to provide informed consent, the legal representative (in these cases, the spouses) provided informed consent while the subject agreed to participation. Fifteen patients with a diagnosis of clinically probable PSP according to NINDS criteria (gradually progressive disorder, age of onset >40 and either vertical supranuclear gaze paresis or both slowing of vertical saccades and prominent postural instability with falls in the first year) [17], were enrolled from the Movement Disorders and Memory Disorders Clinics at University of California, Los Angeles and the Memory and Aging Center at University of California, San Francisco. Subjects underwent examination that included the PSP Rating Scale (PSPRS) [18] and Mini-Mental State Examination (MMSE) [19]. No PSP subject had symptoms of cerebellar ataxia. The subject group consisted of 7 female and 8 male patients aged 59–86 years (mean±SD: 68.3±7.5 years) with duration of disease lasting 2–8 years (mean±SD: 4.7±2.0 years). Eight patients with idiopathic PD with short duration of disease (<5 years, mean 2.4±1.1years) were recruited from the UCLA Movement Disorders Clinic and underwent examination that included the Unified Parkinson Disease Rating Scale (UPDRS) [20] and the MMSE. Demographics for all patient groups are shown in Table 1 (data for individual subjects from all groups are shown in the Supplementary Materials Table S1). Five age matched control subjects without history of neurological disorders and dementia were recruited from a larger study on [F-18]FDDNP PET imaging in aging and AD conducted at UCLA [5].

### PET Imaging Protocol

[F-18]FDDNP was prepared as previously described [21] following currently FDA-mandated regulatory requirements for chemistry, manufacture and control. All PET scans were performed at the UCLA Ahmanson Biomedical Imaging Center using either ECAT HR + PET camera or Biograph PET/CT camera (both Siemens/CTI, Knoxville, TN). Patients lying in supine position on the tomography bed were injected with 10 mCi of [F-18]FDDNP as a bolus intravenous injection following a 10 min attenuation scan. The dynamic data acquisition was started at the time of injection. The following time frames were collected: 6x30 sec, 4x180 sec, and 10x300 sec (total duration: 65 min). All PET scans were decay corrected and reconstructed using filtered back-projection (Hann filter, 5.5 mm FWHM) with scatter correction and measured attenuation correction. The resulting images from the PET camera contained 63 contiguous slices with the plane-to-plane separation of 2.42 mm and images from the PET/CT camera contained 109 contiguous slices with the plane-to-

plane separation of 2.0 mm. No significant differences between images from the two scanners were observed. Motion correction was performed as described previously [22].

### Imaging Analysis

Logan graphical analysis [23] with the cerebellar grey matter as the reference region was performed on dynamic [F-18]FDDNP data sets and parametric images of the distribution volume ratios (DVR) using time frames from 30 min to 65 min were prepared as described previously [4,24]. Cerebellar grey matter is a suitable reference region for analysis of [F-18]FDDNP PET data in PSP subjects since, in the absence of ataxia, only sporadic tau deposition in this area has been observed [25]. No atrophy correction of the PET data was performed. Partial volume effects result in reduction of the PET signal due to brain atrophy and, if performed, this correction would increase the intensity of [F-18]FDDNP brain signal even further.

### [F-18]FDDNP DVR Quantification

Regional [F-18]FDDNP distribution volume ratio (DVR) values were extracted from DVR parametric images using regions-of-interest (ROIs) drawn on the [F-18]FDDNP perfusion image, obtained during the first six minutes of the scan [24]. ROI sets included subcortical areas (striatum, thalamus, subthalamic region, midbrain, cerebellar white matter including deep nuclei, and cortical areas [frontal, parietal, medial temporal (limbic regions, including the hippocampus, parahippocampal areas and entorhinal cortex), lateral temporal and posterior cingulate gyrus]. ROIs were drawn bilaterally on each region, with the exception of the midbrain where only one ROI was placed. Each regional DVR value was calculated as an average of the left and right regions and global cortical DVR values were calculated as averages of the values for all cortical regions (frontal, parietal, medial temporal, lateral temporal and posterior cingulate gyrus).

### Statistical Analysis

ANOVA analysis was conducted to assess whether there were significant differences in regional [F-18]FDDNP binding (DVR values) between PSP, PD, and control groups. Spearman rank correlation ($r_S$) was used to determine the correlation between frontal [F-18]FDDNP DVR values and PSPRS scores in PSP subjects with available PSPRS scores. Student *t*-tests were used to determine whether there were significant differences in regional [F-18]FDDNP binding (DVR values) in all subject groups compared with controls.

## RESULTS

The PSP cohort included four patients with lower MMSE scores in the range of DSM criteria for dementia [21] (MMSE score <25; range 13–23; mean±SD: 18.7±3.3) and nine subjects with higher MMSE scores (MMSE score ≥25; range 25–29; mean±SD: 26.8±1.4) (Supplementary Materials Table S1). The MMSE score was not available for two PSP patients. All PSP patients with MMSE <25 also had high PSPRS scores (range: 41–61; mean±SD: 46.5±9.7) (Supplementary Materials Table S1 and Figure S2).

[F-18]FDDNP binding in PSP subjects differed significantly from that of all other subject groups in several subcortical regions, which are the areas with a higher density of tau aggregates: subthalamic area ($F_{[3,26]} = 33.01$, $P<0.0001$), midbrain region ($F_{[3,26]} = 24.12$, $P<0.0001$), and cerebellar white matter ($F_{[3,26]} = 11.84$, $P<0.0001$) (Figure 1, Figure S3, Table 2). Neocortical regions were affected only in a subset of PSP subjects with more severe clinical symptoms (Table 1) and pattern variability prevalent with binding primarily in the frontal lobe and less frequently in temporal lobes and posterior cingulate gyrus. In the

frontal lobe [F-18]FDDNP binding was correlated with PSPRS score as a measure of severity of symptoms (Figure S4, $r_S = 0.53$, $P<0.05$).

## DISCUSSION

The observed patterns of subcortical [F-18]FDDNP binding in PSP (Figure 2) correlated well with (i) known patterns of brain areas frequently affected by different subtypes of tau aggregates (NFTs, tufted astrocytes, coiled bodies) throughout PSP disease progression, and (ii) symptomatology, as motor symptoms are typically more prominent in this disease. Variable patterns of cortical [F-18]FDDNP binding, e.g., frontal lobe (Figure S4), were observed in PSP subjects, with higher levels observed in patients with more severe disease. Especially in the earliest states of PSP, [F-18]FDDNP brain imaging shows distinctive differences in subcortical areas compared with early PD, with which it may be overlapping clinically (Figures 2 and 3). Early in disease presentation subjects with PSP are often misdiagnosed with PD given the similarity in syndromes with patients exhibiting bradykinesia, rigidity, and gait and postural instability. Only after disease progression will the diagnosis of PSP become more certain. Comparing this pattern with the patterns of [F-18]FDDNP binding in other neurodegenerative diseases, it is clear that [F-18]FDDNP binding in the subthalamic area, midbrain and cerebellar areas is specific to PSP and not observed in other disorders and thus, could be a valuable diagnostic aid. Earlier diagnosis is critical particularly as tau-specific therapies become available in the future.

As stated earlier, only [F-18]FDDNP has currently the ability to visualize *in vivo* tau-aggregate-rich brain regions in patients with AD (i.e., medial temporal lobe) [4,5] and tau-positive frontotemporal dementia (frontal and temporal lobes) [8]. The ability of [F-18]FDDNP to label both β-amyloid and hyperphosphorylated tau aggregates in AD is based on the recognition of β-pleated sheet secondary structures in rigid fibrils present in both types of pathological protein deposits. Additional *in vitro* line of evidence supporting FDDNP tau binding includes co-crystallization of the DDNP moiety with VQIVYK segments from the tau protein repeat domain at atomic resolution [27] (Figure 4), [F-18]FDDNP binding to K183K280 tau fibrils ($K_D = 36.7 \pm 11.6$ nM) [10], FDDNP labeling of cells transfected with SY5Y tau constructs, and tau aggregates in NFTs in MAPT transgenic mice, both detected by fluorescence microscopy (Cole et al, unpublished observations), as well as tau labeling in AD brain specimens [5]. With the apparent exception of globose neurofibrillary tangles [3], these *in vitro* and *in vivo* results demonstrate the ability of the 2-dicyanopropenyl-6-dialkylaminonaphthalene scaffold to bind tightly to structures formed by tau fragments.

Our findings with PSP subjects suggest that [F-18]FDDNP offers promise as a tool in the clinical evaluation of patients with neurodegenerative diseases including the tauopathies. These disorders are characterized by a spectrum of clinical symptoms ranging from motor dysfunction to dementia as a result of extensive neuronal loss in specific vulnerable neuronal populations [28]. Observed differences in clinical presentation of various tauopathies are based on structural, physiological and functional alterations of different brain circuits brought forth by underlying cellular and tau-induced degenerative changes. Although the relationships among these tau pathological changes, neuronal loss and clinical symptoms are complex and not well understood, it is clear that hyperphosphorylation of tau proteins, their polymerization and formation of cellular inclusions is required for full disease evolution. [29, 30].

Neuropathology reports in PSP have shown that the subthalamic nucleus, substantia nigra (midbrain) and globus pallidus internus are consistently affected, even in cases with the mildest clinical symptoms and the lowest lesion burden [15]. Analysis of different cellular

types of tau aggregates has revealed that all types found commonly in PSP, i.e., neurofibrillary tangles, tufted astrocytes and coiled bodies in oligodendrocytes, are composed of straight fibrils formed predominatly by four repeat isoforms [31]. Total tau pathology load varies considerably among brain regions and within patients with PSP. NFTs are most abundant in the basal ganglia and brainstem structures; tufted astrocytes are most abundant in the cortices, putamen and caudate nucleus; and coiled bodies and tau threads, which are the major contributors to the overall tau load, are most numerous in the subthalamic nucleus, substantia nigra and globus pallidus internus and least dense in cortical regions [15]. This is again entirely consistent with the observed [F-18]FDDNP brain distribution observed in the living brain of these patients and [F-18]FDDNP's ability to detect four repeat isoforms of these tau fibrillar aggregates.

In addition to typical PSP as defined by NINDS clinical [17] and neuropathological [32] criteria, up to six atypical subtypes have been described. These can be largely subdivided into cortical predominant and brain stem predominant PSP subtypes [30]. Regardless of its clinical variability, early pathology deposition in PSP seems to occur first in a progressive fashion in subcortical areas, most specifically in globus pallidus, subthalamic structures, brain stem and cerebellar white matter spreading to the cortex in later stages of the disease. Observations with this PSP patient population reveal consistent [F-18]FDDNP subcortical involvement and a variable pattern of cortical involvement possibly reflecting different pathological stages of the disease (Table 2), which is evident as increased [F-18]FDDNP binding in cortical areas is observed in more symptomatic PSP subjects (higher PSPRS score)(Figure S4). Although symptoms included in PSPRS score are not cortical they serve as indication of disease severity. In the absence of pathology results from these more affected subjects it is not possible to exclude the presence of concurrent AD pathology in some of the PSP subjects presenting cortical [F-18]FDDNP binding.

Figure 2 and Table 2 demonstrate the different [F-18]FDDNP distribution reflecting the differential patterns of subcortical binding in PSP and PD. This consistent subcortical [F-18]FDDNP binding to tau pathological aggregates may be of help to clinicians in the differential diagnosis of PSP, even the PSP-Parkinsonism variant, and PD [15]. These findings confirm previous reports on *in vivo* [F-18]FDDNP imaging of tau fibrillar deposits [33, 34], but the small number of PSP subjects in this intial study and the lack of confirmed pathology in these subjects present a limitation for a more general interpretation of the imaging results. However, recent work on [F-18]FDDNP imaging with retired football players with possible chronic traumatic encephalopathy (CTE) [35] offers confirmatory evidence of the utility of [F-18]FDDNP as an *in vivo* tau marker in neurodegenerative tauopathies, with sufficient sensitivity to detect variable patterns of regional tau pathology load. On a more general note, this work with PSP subjects also demonstrates that the pi-conjugation of a dialkylamino group, as the electron donor, with a 2-cyano acrylate unit in the dialkylamino naphthalenyl-2-cyanoacrylate motif, as the electron acceptor (e.g., in 2-dicyanopropenyl-6-dialkylaminonaphthalenes as [F-18]FDDNP), does produce tau-binding molecules with significant sensitivity for *in vivo* detection of tau aggregation in humans. Of importance is that the tau binding properties of such a motif as well as its specificity for tau (e.g., vs. Aβ binding) could be fine-tuned by modifying the electronic density and extent of conjugation between the donor and acceptor units. This approach offers a framework for the development and testing of new neurofibrillary tau specific imaging probes in parallel with X-ray microcrystallography at atomic resolution in co-crystallization experiments [27].

## Supplementary Material

Refer to Web version on PubMed Central for supplementary material.

## Acknowledgments

Supported by National Institutes of Health (P01-AG025831, R01AG038791, R01AG031278, R01AG034499, P50 AG 16570) and by the Tau Research Consortium. JRB gratefully acknowledges support from the Elizabeth and Thomas Plott Endowment in Gerontology. No company provided support of any kind for this study. Special thanks also to N. Satyamurthy and cyclotron staff and J. Williams and the Nuclear Medicine Clinic staff for their support with the scanning protocols.

## References

1. Small GW, Bookheimer SY, Thompson PM, Cole GM, Huang SC, Kepe V, Barrio JR. Current and future uses of neuroimaging for cognitively impaired patients. Lancet Neurol. 2008; 7:161–172. [PubMed: 18207114]
2. Rowe CC, Villemagne V. Brain amyloid imaging. J Nucl Med. 2011; 52:1733–1740. [PubMed: 21917849]
3. Smid LM, Vovko TD, Popovic M, Petric A, Kepe V, Barrio JR, Vidmar G, Bresjanac M. The 2,6-disubstituted naphthalene derivative FDDNP labeling reliably predicts Congo red birefringence of protein deposits in brain sections of selected human neurodegenerative diseases. Brain Pathol. 2006; 16:124–130. [PubMed: 16768752]
4. Shoghi-Jadid K, Small GW, Agdeppa ED, Kepe V, Ercoli LM, Siddarth P, Read S, Satyamurthy N, Petric A, Huang SC, Barrio JR. Localization of neurofibrillary tangles and beta-amyloid plaques in the brains of living patients with Alzheimer disease. Am J Geriatr Psychiatry. 2002; 10:24–35. [PubMed: 11790632]
5. Small GW, Kepe V, Ercoli LM, Siddarth P, Bookheimer SY, Miller KJ, Lavretsky H, Burggren AC, Cole GM, Vinters HV, Thompson PM, Huang SC, Satyamurthy N, Phelps ME, Barrio JR. PET of brain amyloid and tau in mild cognitive impairment. N Engl J Med. 2006; 355:2652–2663. [PubMed: 17182990]
6. Boxer AL, Rabinovici GD, Kepe V, Goldman J, Furst AJ, Huang SC, Baker SL, O'neil JP, Chui H, Geschwind MD, Small GW, Barrio JR, Jagust W, Miller BL. Amyloid imaging in distinguishing atypical prion disease from Alzheimer disease. Neurology. 2007; 69:283–290. [PubMed: 17636066]
7. Kepe V, Ghetti B, Farlow MR, Bresjanac M, Miller K, Huang SC, Wong KP, Murrell JR, Piccardo P, Epperson F, Repovs G, Smid LM, Petric A, Siddarth P, Liu J, Satyamurthy N, Small GW, Barrio JR. PET of brain prion protein amyloid in Gerstmann-Sträussler-Scheinker disease. Brain Pathol. 2010; 20:419–430. [PubMed: 19725833]
8. Barrio JR, Satyamurthy N, Huang SC, Petric A, Small GW, Kepe V. Dissecting molecular mechanisms in the living brain of dementia patients. Acc Chem Res. 2009; 42:842–850. [PubMed: 19281227]
9. Fodero-Tavoletti MT, Okamura N, Furumoto S, Mulligan RS, Connor AR, McLean CA, Cao D, Rigopoulos A, Cartwright GA, O'Keefe G, Gong S, Adlard PA, Barnham KJ, Rowe CC, Masters CL, Kudo Y, Cappai R, Yanai K, Villemagne VL. 18F-THK523: a novel in vivo tau imaging ligand for Alzheimer's disease. Brain. 2011; 134:1089–1100. [PubMed: 21436112]
10. Harada R, Okamura N, Furumoto S, Tago T, Maruyama M, Higuchi M, Yoshikawa T, Arai H, Iwata R, Kudo Y, Yanai K. Comparison of the binding characteristics of [18F]THK-523 and other amyloid imaging tracers to Alzheimer's disease pathology. Eur J Nucl Med Mol Imaging. 2013; 40:125–132. [PubMed: 23100049]
11. Xia CF, Arteaga J, Chen G, Gangadharmath U, Gomez LF, Kasi D, Lam C, Liang Q, Liu C, Mocharla VP, Mu F, Sinha A, Su H, Szardenings AK, Walsh JC, Wang E, Yu C, Zhang W, Zhao T, Kolb HC. [(18)F]T807, a novel tau positron emission tomography imaging agent for Alzheimer's disease. Alzheimers Dement. 2013 [Epub]. 10.1016/j.jalz.2012.11.008
12. Villemagne V, Furumoto S, Fodero-Tavoletti M, Mulligan R, Hodges J, Kudo Y, Masters C, Yanai K, Rowe C, Okamura N. In vivo tau imaging in Alzheimer's disease. J Nucl Med. 2012; 53(Suppl1):36.
13. Chien DT, Bahri S, Szardenings AK, Walsh JC, Mu F, Su MY, Shankle WR, Elizarov A, Kolb HC. Early Clinical PET Imaging Results with the Novel PHF-Tau Radioligand [F-18]-T807. J Alzheimers Dis. 2013; 34:457–468. [PubMed: 23234879]

14. Tolnay M, Probst A. The neuropathological spectrum of neurodegenerative tauopathies. IUBMB Life. 2003; 55:299–305. [PubMed: 12938731]
15. Williams DR, Holton JL, Strand C, Pittman A, de Silva R, Lees AJ, Revesz T. Pathological tau burden and distribution distinguishes progressive supranuclear palsy-parkinsonism from Richardson's syndrome. Brain. 2007; 130:1566–1576. [PubMed: 17525140]
16. Armstrong RA, Lantos PL, Cairns NJ. Progressive supranuclear palsy (PSP): a quantitative study of the pathological changes in cortical and subcortical regions of eight cases. J Neural Transm. 2007; 114:1569–1577. [PubMed: 17680229]
17. Litvan I, Agid Y, Calne D, Campbell G, Dubois B, Duvoisin RC, Goetz CG, Golbe LI, Grafman J, Growdon JH, Hallett M, Jankovic J, Quinn NP, Tolosa E, Zee DS. Clinical research criteria for the diagnosis of progressive supranuclear palsy (Steele-Richardson-Olszewski syndrome): report of the NINDS-SPSP international workshop. Neurology. 1996; 47:1–9. [PubMed: 8710059]
18. Golbe LI, Ohman-Strickland PA. A clinical rating scale for progressive supranuclear palsy. Brain. 2007; 130:1552–1565. [PubMed: 17405767]
19. Folstein MF, Folstein SE, McHugh PR. "Mini-mental state": a practical method for grading the cognitive state of patients for the clinician. J Psychiatr Res. 1975; 12:189–198. [PubMed: 1202204]
20. Fahn, S.; Elton, RL. the UPDRS Development Committee. Unified Parkinson's Disease Rating Scale. In: Fahn, S.; Marsden, CD.; Calne, D.; Goldstein, M., editors. Recent Developments in Parkinson's Disease. Vol. 2. Macmillan Healthcare Information; Florham Park, NJ: 1987. p. 153-163.
21. Liu J, Kepe V, Zabjek A, Petric A, Padgett HC, Satyamurthy N, Barrio JR. High-yield, automated radiosynthesis of 2-(1-{6-[(2-[$^{18}$F]fluoroethyl)(methyl)amino]-2-naphthyl}ethylidene)malononitrile ([$^{18}$F]FDDNP) ready for animal or human administration. Mol Imaging Biol. 2007; 9:6–16. [PubMed: 17051324]
22. Wardak M, Wong KP, Shao W, Dahlbom M, Kepe V, Satyamurthy N, Small GW, Barrio JR, Huang SC. Movement correction method for human brain PET images: application to quantitative analysis of dynamic 18F-FDDNP scans. J Nucl Med. 2010; 51:210–218. [PubMed: 20080894]
23. Logan J, Fowler JS, Volkow ND, Wang GJ, Ding YS, Alexoff DL. Distribution volume ratios without blood sampling from graphical analysis of PET data. J Cereb Blood Flow Metab. 1996; 16:834–840. [PubMed: 8784228]
24. Kepe V, Huang SC, Small GW, Satyamurthy N, Barrio JR. Visualizing pathology deposits in the living brain of patients with Alzheimer's disease. Methods Enzymol. 2006; 412:144–160. [PubMed: 17046657]
25. Jellinger K. Cerebellar involvement in progressive supranuclear palsy. Mov Disord. 2010; 25:1104–1105. [PubMed: 20222135]
26. American Psychiatric Association. Diagnostic and Statistical Manual of Mental Disorders. 4. American Psychiatric Association; Washington, DC: 2000. Text Revision
27. Landau M, Sawaya MR, Faull KF, Laganowsky A, Jiang L, Sievers SA, Liu J, Barrio JR, Eisenberg D. Towards the amyloid pharmacophore. PLoS Biology. 2011; 9:e1001080. [PubMed: 21695112]
28. Lee VM, Goedert M, Trojanowski JQ. Neurodegenerative tauopathies. Annu Rev Neurosci. 2001; 24:1121–1159. [PubMed: 11520930]
29. von Bergen M, Friedhoff P, Biernat J, Heberle J, Mandelkow EM, Mandelkow E. Assembly of tau protein into Alzheimer paired helical filaments depends on a local sequence motif ((306)VQIVYK (311)) forming beta structure. Proc Natl Acad Sci USA. 2010; 97:5129–5134. [PubMed: 10805776]
30. Dickson DW, Ahmed Z, Algom AA, Tsuboi Y, Josephs KA. Neuropathology of variants of progressive supranuclear palsy. Curr Opin Neurol. 2010; 23:394–400. [PubMed: 20610990]
31. Arima K. Ultrastructural characteristics of tau filaments in tauopathies: immuno-electron microscopic demonstration of tau filaments in tauopathies. Neuropathology. 2006; 26:475–483. [PubMed: 17080728]

32. Hauw JJ, Daniel SE, Dickson D, Horoupian DS, Jellinger K, Lantos PL, McKee A, Tabaton M, Litvan I. Preliminary NINDS neuropathologic criteria for Steele-Richardson-Olszewski syndrome (progressive supranuclear palsy). Neurology. 1994; 44:2015–2019. [PubMed: 7969952]

33. Barrio, JR.; Bordelon, Y.; Small, GW.; Kepe, V. Visualizing tau pathology in the living brain of progressive supranuclear palsy patients, AD/PD 2011. Barcelona, Spain: 2011.

34. Shin J, Kepe V, Small GW, Phelps ME, Barrio JR. Multimodal imaging of Alzheimer pathophysiology in the brain's default mode network. Int J Alzheimer's Dis. 2011; 2011:687945. [PubMed: 21629709]

35. Small GW, Kepe V, Siddarth P, Ercoli LM, Merrill DA, Donoghue N, Bookheimer SY, Martinez J, Omalu B, Bailes J, Barrio JR. PET Scanning of Brain Tau in Retired National Football League Players: Preliminary Findings. Am J Geriatr Psychiatry. 2013; 21:138–144. [PubMed: 23343487]

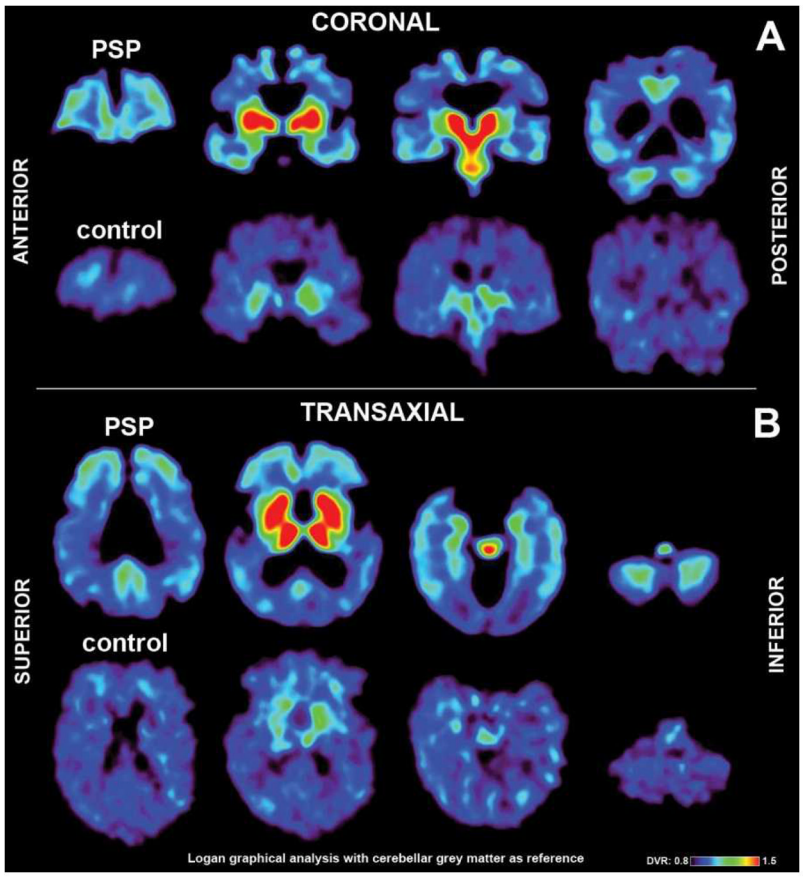


**Figure 1.**

Coronal (A) and transaxial (B) brain [F-18]FDDNP DVR images sections of human subjects showing the distribution of [F-18]FDDNP DVR signal in a PSP subject (PSP12; upper row in each view) and a typical control (CTRL3; lower row in each view). DVR values are normalized to cerebellar grey matter. Highest [F-18]FDDNP signal in PSP subject is observed in striatum, thalamus, sub-thalamic region, midbrain, pons and cerebellar white matter. Cortical signal, when present, is predominantly in frontal areas, but can be also present in temporal areas and posterior cingulate gyrus. Since total cortical tau load reflects all three pathology subtypes (tufted astrocytes, coiled bodies and neurofibrillary tangles), which have different distribution patterns and densities (for examples see Supplementary Materials Figure S1), it is not surprising that patterns of cortical [F-18]FDDNP signal can vary significantly among PSP subjects (Tables 2 and S2).

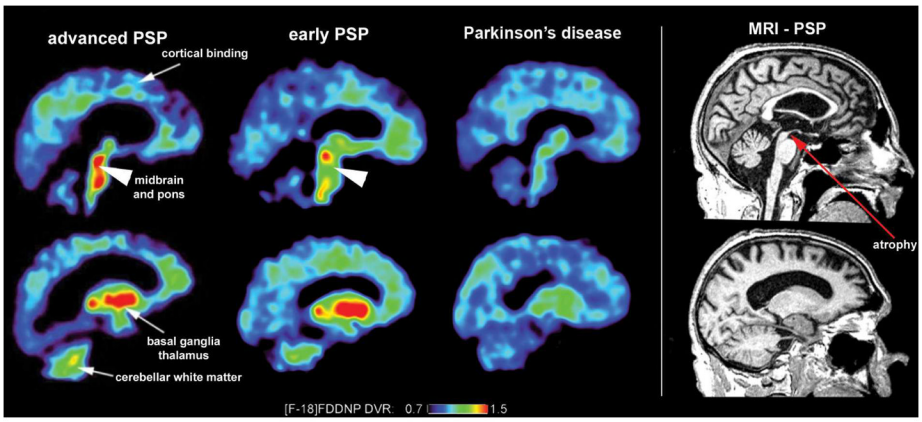


**Figure 2.**

Representative examples of [F-18]FDDNP binding patterns observed in PSP with longer duration (advanced PSP, left column), in PSP with shorter duration without cortical signal (early PSP, middle column), and in Parkinson's disease (right column). PSP and PD conditions can overlap at early stages in their symptomatology but can be distinguished based on the pattern of [F-18]FDDNP DVR binding. [F-18]FDDNP signal in subthalamic region, in midbrain and in cerebellar white matter is elevated even in PSP subjects at early stages of disease but not in Parkinson's disease subjects (also see Table 2). The areas with high [F-18]FDDNP DVR signal are known to be affected by PSP as shown by MRI where significant midbrain atrophy is obvious.

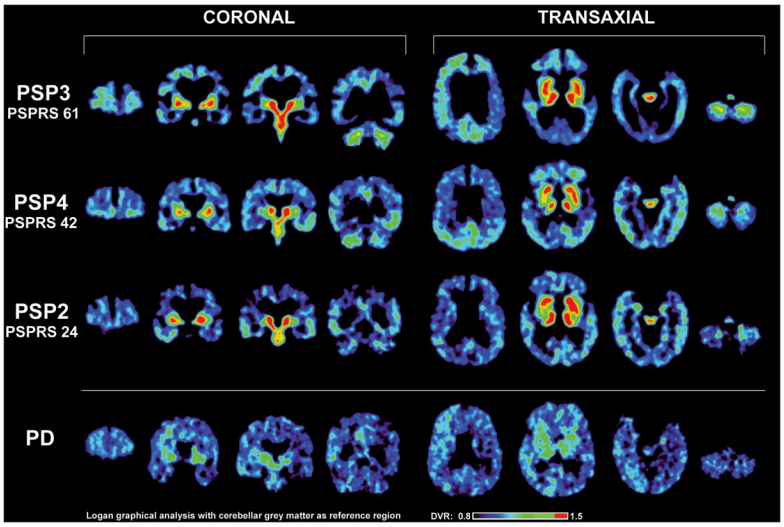


**Figure 3.**
Detailed views of [F-18]FDDNP DVR parametric images shown in coronal and transaxial orientation are shown for three PSP patients. PD5 subject is shown for comparison. Subthalamic areas are indicated by arrowheads.

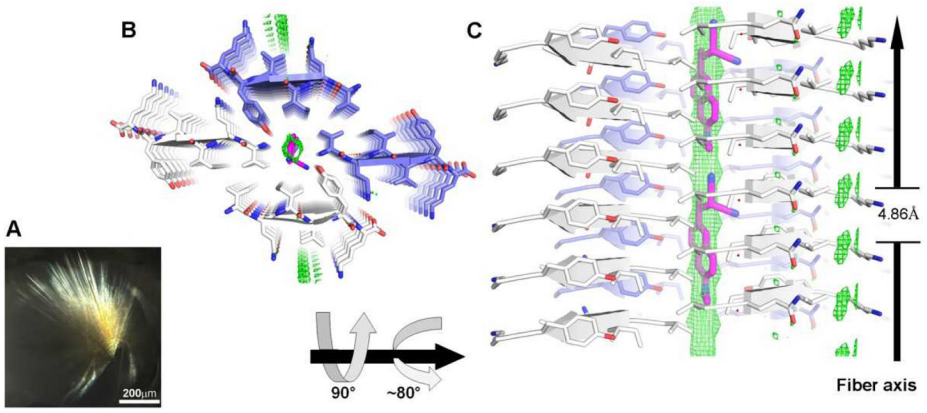


**Figure 4.**

Models of DDNP bound to a tau segment (VQIVYK fiber) based on undifferentiated electron density. Panel A shows micro-crystals of VQIVYK co-crystallized with DDNP. In the structure of the complexes with DDNP (**B–C**), VQIVYK is packed in a form having a steric zipper with one β-sheet shifted in relation to the other β-sheet (cartoon arrows). Six layers of the fiber are depicted. In panel **B** the view looks down the fiber axis. In Panel **C** the view is perpendicular to the fiber axis. DDNP (**B–C,** two molecules are shown) has been computationally docked into the structures and fit the location of the positive density. The unit cell dimension of the crystal along the fiber axis is indicated. The length of DDNP spans multiple unit cells of the fibril; that is, the dimensions of the small molecule and the fibril unit cell are incommensurate (From Landau et al,[21] PLoS Biol, 2011;9:e1001080, Epub 2011 Jun 14, with permission).

**Table 1**

Cumulative demographic and clinical data for PSP, PD, and control subject groups.

| Subject | Age (years) | Gender | Disease Duration (years) | MMSE Score | PSPRS Score | Motor UPDRS |
|---|---|---|---|---|---|---|
| **PSP (n=15)** | 68.3±7.5 | 7F / 8M | 4.7±2.0 | 24.3±4.6 | 42.4±9.5 | N/A |
| **PD (n=8)** | 57.9±10.0 | 4F / 4M | 2.4±1.1 | 28.5±2.3 | N/A | 13.1±6.7 |
| **Control (n=5)** | 68.0±8.6 | 2F / 3M | N/A | 29.6±0.5 | N/A | N/A |

N/A: Not applicable

**Table 2**

**Regional [F-18]FDDNP DVR values**

Note high [F-18]FDDNP DVR values in subthalamic area, midbrain and cerebellar white matter, which are not present in thePD subject group, and which could serve as [F-18]FDDNP PET measures for diagnosis of PSP.

| Subject | Frontal | Parietal | Medial Temporal | Lateral Temporal | Posterior Cingulate | Striatum | Thalamus | STA | Midbrain | WM/C |
|---|---|---|---|---|---|---|---|---|---|---|
| **PSP** (mean±SD) | 1.065±0.058 | 1.075±0.057 | 1.090±0.068 | 1.106±0.065// | 1.161±0.080// | **1.443±0.102**† | **1.478±0.070**‡ | **1.434±0.070**‡ | **1.367±0.079**‡ | **1.209±0.080**‡ |
| **PD** (mean±SD) | 1.033±0.052 | 1.040±0.029 | 1.037±0.080 | 1.075±0.036 | 1.028±0.040 | 1.206±0.115 | 1.210±0.093 | 1.211±0.070 | 1.127±0.071 | 1.021±0.066 |
| **Control** (mean±SD) | 1.038±0.018 | 1.069±0.020 | 1.109±0.020 | 1.76±0.017 | 1.090±0.048 | 1.250±0.082 | 1.250±0.045 | 1.233±0.036 | 1.167±0.051 | 1.076±0.018 |
| **PSP** (Z score) | 1.50 | 0.30 | −0.95 | 1.76// | 1.48// | **2.35**† | **5.07**‡ | **5.58**‡ | **3.92**‡ | **7.38**‡ |
| **PD** (Z score) | −0.27 | −1.45// | −3.60// | −0.06 | −1.29// | −0.54 | −0.89 | −0.61 | −1.24 | 0.67 |

STA: sub-thalamic area; WM/C: cerebellar white matter.

Group mean [F-18]FDDNP DVR values for five subcortical and five cortical brain areas shown for PSP subjects (n=15), Parkinson's disease group (n=8), and controls (N=5). Z scores are in reference to the mean values for the control group in each area.

Values which were also significantly different from PD subject group (ANOVA) are shown in bold. Student *t*-test for comparison with the control group;

*P* values:

//<0.05,

†<0.005,

‡<0.001.